BEAM COLLIMATION AND MACHINE-DETECTOR INTERFACE AT THE INTERNATIONAL LINEAR COLLIDER[*]

N.V. Mokhov[†], A.I. Drozhdin, M.A. Kostin, FNAL, Batavia, IL 60510, USA

Abstract

Synchrotron radiation, beam-gas scattering and beam halo interactions with collimators and other components in the ILC beam delivery system (BDS) would create fluxes of muons and other secondaries which could exceed the tolerable levels at a detector by a few orders of magnitude. It is shown that with a multi-stage collimation system and magnetized iron spoilers which fill the tunnel one can meet the design goals. Results of modeling with the STRUCT [1] and MARS15 [2] codes of beam loss and energy deposition effects are presented in this paper. We focus on the collimation system and mask performance optimization, short- and long-term survivability of the critical components (spoilers, absorbers and magnets), dynamic heat loads and radiation levels in magnets and other components, and machine-related backgrounds in collider detectors.

BEAM PARAMETERS AND ASSUMPTIONS

For simulation of the ILC (Table 1) collimation system efficiency, the beam halo was represented by 10^6 rays with $1/x$ and $1/y$ density distributions on betatron amplitudes in the range $A_x = (5\text{-}13)\sigma_x$ and $A_y = (36\text{-}93)\sigma_y$, with the Gaussian momentum distribution $\sigma(\Delta p/p) = 1\%$. The amplitude range was chosen to appropriately overlap the design collimation depth. Such a halo distribution maximizes the fraction of particles that can interact with the spoiler edges, producing large number of out-scattered particles from the spoilers. It is a more pessimistic assumption than, for example, a uniformly distributed halo with the same maximal range. All results below are normalized to 0.1% of the beam intensity in the halo hitting the collimators.

COLLIMATION SYSTEM PERFORMANCE

The collimation system is intended to localize the beam loss in a specially equipped part of the BDS to minimize particle loss in the IP region. The philosophy of the collimation is to use large aperture magnets and collimate the beam at largest possible amplitudes to avoid excessive production of muons. Besides, it is well understood that the synchrotron radiation photons produced by the beam halo in the final focus doublet upstream of the IP should pass

---

Table 1: ILC beam parameters.

parameter	ILC-500
Center of mass energy, GeV	500
Number of particles per bunch	2×10^{10}
Number of bunches per train	2820
Separation between bunches, ns	337
Repetition frequency, Hz	5
Average current (each beam), μA	45.1
Beam power (each beam), MW	11.3
Normal. emitt. x,y, mm·mrad	10, 0.03
Beta function at IP, x,y, mm	15.233, 0.408
Beam size at IP, x,y, (σ), nm	553, 5
Fractional halo on collimators	0.1%

freely through the aperture of the elements on the opposite side of the IP. This requires to keep the beam halo size in the final doublet at $9\sigma_x$ and $65\sigma_y$.
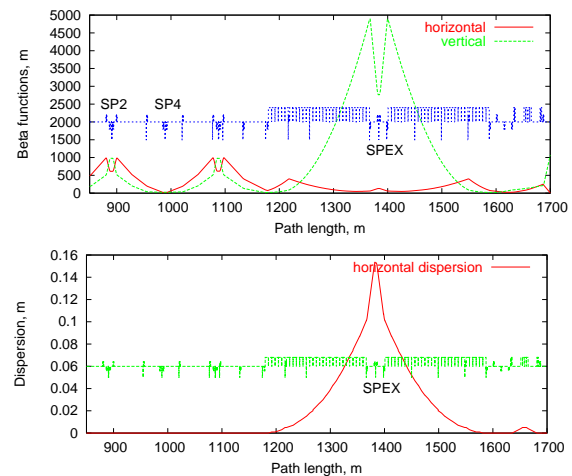

Figure 1: $\beta_{x,y}$ and dispersion in the collimation region.

To reduce energy deposition density in primary collimators (betatron spoilers SP2, SP4) they are located in high-$\beta_{x,y}$ regions (Fig. 1) with a $90°$ phase advance between them. The off-momentum spoiler SPEX is in a high dispersion region, where off-momentum particles can be safely absorbed. The betatron spoilers are 0.6 X_0 (radiation length) thick, momentum spoiler is 1 X_0, absorbers and synchrotron radiation masks (MSK1,2) are 30 X_0, and electron masks (PC) are 15 X_0. The spoilers are located at $8\sigma_x$ and $65\sigma_y$. To prevent damage of the BDS components, the halo particles are allowed to interact only with thin spoilers, with all the thick collimators positioned farther from the beam at $>16\sigma_x$ and $>150\sigma_y$.
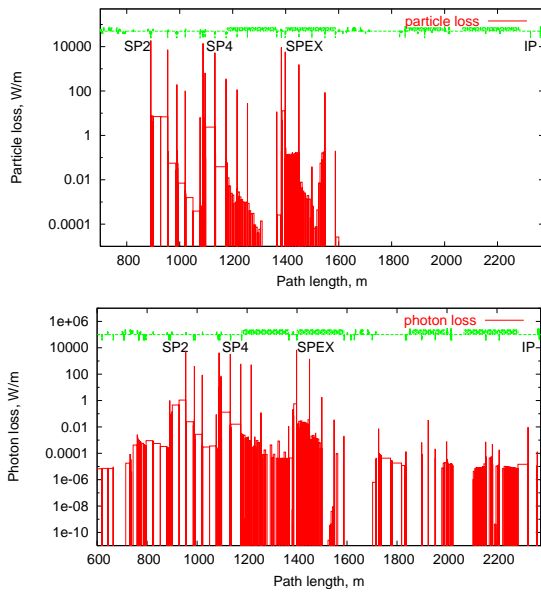
Figure 2: Electron (top) and photon (bottom) loss in BDS.

Calculated electron and photon losses in the BDS are presented in Fig. 2. Power of bremsstrahlung photons and secondary electrons generated in the spoilers, and then intercepted by the collimators are shown in Table 2 for various collimator apertures. The bremsstrahlung photons contribute ~50% of the total power.

Table 2: Photon and secondary particle loss on selected collimators with a tight collimator aperture (~1 mm) and enlarged apertures.

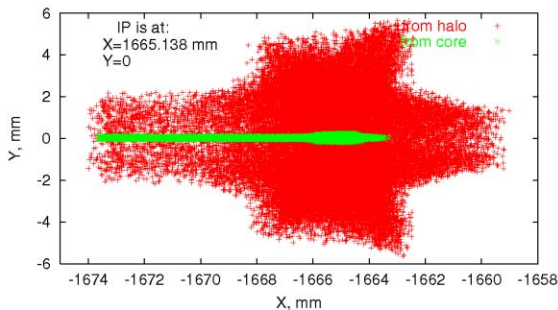|	Path	tight	$\gamma + e^- + e^+$ power, W			
	length	posit. x/y	collimator position			
element	m	mm/mm	tight	3 mm	4 mm	5 mm
PC1	954.7	1.3/0.7	2707	1331	869	552
PC2	1020.7	1.1/0.7	40	372	392	368
PC3	1076.9	2.8/1.5	1.4	208	248	259
PC5	1133.0	1.8/0.7	1845	693	404	239
PC6	1216.7	1.8/0.7	132	786	910	924
PC8	1398.4	0.7/0.7	2626	627	317	186
PC9	1450.1	0.7/1.2	617	2258	2299	2153

Figure 3: Transverse distribution of photons at IP from beam halo and core.

Characteristics of photons lost on masks MSK1 and MSK2 at 50 m and 13 m from the IP, on PDUMP and those passed through the detector aperture are shown in Table 3.

Table 3: Characteristics of photons lost on PDUMP, MSK1, MSK2 and passed through IP.

element	Mean energy GeV	Photons number per bunch	Photon energy per bunch GeV/bunch
synchrotron radiation from beam halo			
lost at PDUMP	0.752E-04	0.373E+07	0.280E+03
lost at MSK1	0.155E-03	0.115E+07	0.179E+03
lost at MSK2	0.300E-04	0.768E+05	0.230E+01
pass through IP	0.320E-02	0.422E+07	0.135E+05
bremsstrahlung photons from beam halo			
lost at PDUMP, MSK1, MSK2	0	0	0
pass through IP	0.140E+00	0.400E+03	0.561E+02
synchrotron radiation from beam core			
lost at PDUMP	0.740E-04	0.426E+10	0.315E+06
lost at MSK1	0.683E-04	0.464E+10	0.317E+06
lost at MSK2	0.305E-04	0.396E+09	0.121E+05
pass through IP	0.398E-03	0.383E+10	0.152E+07

Synchrotron radiation power intercepted by the masks from halo is three order of magnitude less compared to that from the beam core. Transverse profiles of photons generated by the beam halo and core are presented in Fig. 3. The narrow core-related distribution is emitted in the last bending magnets located at 90 m upstream the IP. All photons generated on the masks have energy below 0.5 MeV, while photons passing through the IP are in the 1 to 100 MeV range.
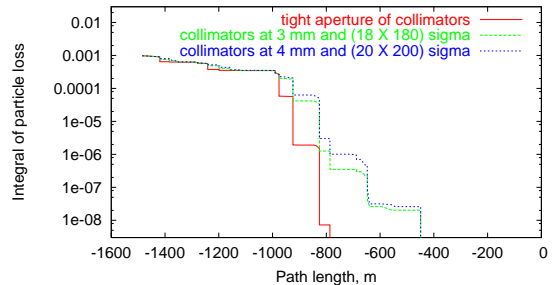

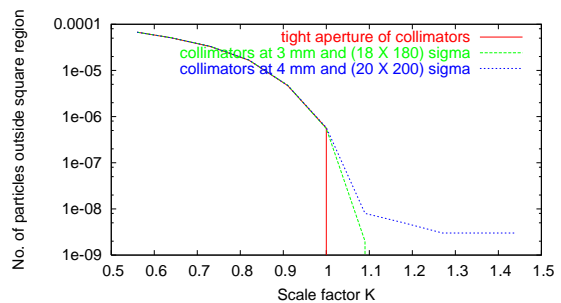Figure 4: Collimation system efficiency.

Figure 5: Number of charged-halo particles in a rectangular x-y window at the entrance to the final doublet.

The collimation system efficiency is presented in Fig. 4, where a fractional loss of charged-halo particles, integrated back, starting at the IP, and normalized to the nominal bunch charge are shown. The number of charged-halo particles per bunch, normalized to the nominal bunch charge, in a rectangular x-y window at the entrance to the final dou-

blet, is shown in Fig 5. The scale factor K defines the window: for K=1, the window corresponds to the collimation requirements. Three cases are presented in both figures: tight collimator aperture (∼1 mm) and larger apertures of 3 and 4 mm.

RADIATION LOADS IN BDS

Energy deposition effects in the BDS and muon backgrounds on a collider detector were simulated with the MARS15 code [2]. The model includes all the BDS elements with their geometry, materials and magnetic fields as well as a tunnel with concrete walls surrounded by dirt. Phase coordinates of particles lost on the spoilers - as described in previous section - are taken from the STRUCT runs. The reference orbit and phase space propagation calculated with MARS15 coincide with those from STRUCT. Main features of MARS dynamic heat load distributions are similar to those shown in Fig. 2, although details and values are somewhat different because of the difference in the cutoff energies: 0.1 MeV in MARS with full shower modeling and 5 GeV in STRUCT. MARS gives about 50 W/m for the spoilers SP2, SP4 and SPEX, and much higher values - up to 10 kW/m - for the masks PC1, PC5, PC8 and PC9.

The hottest BDS element besides the collimators is the first quadrupole downstream of PC1. Fig. 6 shows absorbed dose isocontours on its upstream end. The peak dose in the coils exceeds 100 MGy/yr to be compared to the epoxy radiation damage limit of 4 MGy. Obviously, further optimization of protection collimators is needed including increase of their lengths from 0.2 m to about 0.4 m, and one should consider use of non-organic insulation for the quadrupoles in such hot spots. Residual dose rate on the upstream end of the above quadrupole is 8.6 mSv/hr and can be reduced to a desirable level of <1 mSv/hr with longer protection collimators.

Depending on the site, the ground water activation limits outside the tunnel at the locations of the hottest masks can be exceeded. To provide the adequate ground water protection, one needs to surround these elements with shielding.

MUON BACKGROUNDS

A lot of muons are generated - predominantly as Bethe-Heitler pairs - in electromagnetic showers induced in the collimators and other BDS elements during the beam halo cleaning. Fluxes of these muons accompanied by other secondary particles, could exceed the tolerable levels at the detector by a few orders of magnitude. Fig. 7 shows muon flux isocontours on the detector from one beam. On average, it equals to 4.1 cm^{-2}s^{-1}, or 7600 muons in the tunnel aperture for 150 bunches. The flux doubles for energetic muons for two beams. The mean energy of these muons is about 27 GeV.

Magnetized spoilers in the tunnel would reduce muon fluxes substantially [3]. MARS calculations were performed for two iron spoilers 9 and 18 m thick at 648 and 331 m
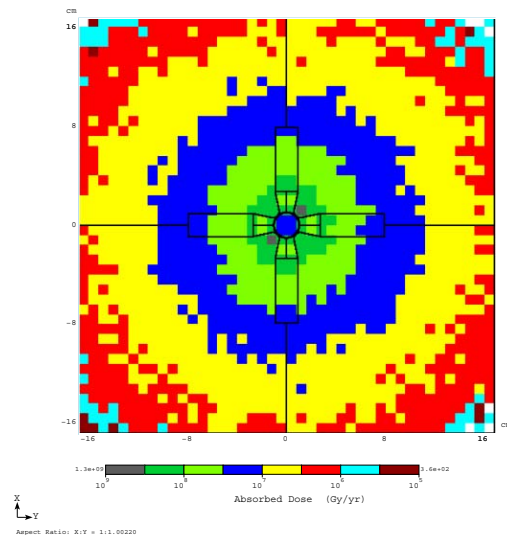

Figure 6: Absorbed dose isocontours in the quadrupole downstream of the mask PC1.

from the IP, respectively. The square spoilers are extended by 0.6 m in the tunnel walls and dirt on each side. The field of 1.5 T is used in opposite polarity on left and right sides to compensate it at the beam pipe center. Preliminary results show that the muon fluxes at the detector are reduced by almost a factor of 8000 to about 1 muon in the tunnel aperture for 150 bunches.
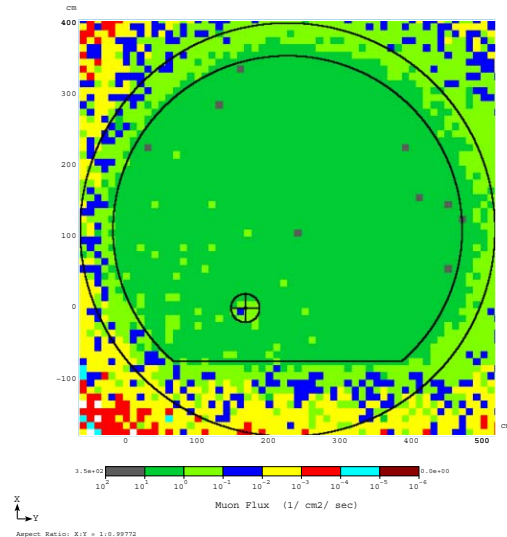

Figure 7: Muon flux isocontours on the detector.

REFERENCES

[1] A.I. Drozhdin, et al. "STRUCT Program User's Reference Manual", http://www-ap.fnal.gov/users/drozhdin/

[2] N.V. Mokhov, "The MARS Code System User's Guide", Fermilab-FN-628 (1995); N.V. Mokhov, et al, "Recent Enhancements to the MARS15 Code", Fermilab-Conf-04/053 (2004); http://www-ap.fnal.gov/MARS/.

[3] Lew Keller, private communication.